AMERICAN SOCIETY FOR MICROBIOLOGY | Applied and Environmental Microbiology

Heat Stress Modulates Mycelium Growth, Heat Shock Protein Expression, Ganoderic Acid Biosynthesis, and Hyphal Branching of *Ganoderma lucidum* via Cytosolic Ca^{2+}

Xue Zhang, Ang Ren, Meng-Jiao Li, Peng-Fei Cao, Tian-Xi Chen, Guang Zhang, Liang Shi, Ai-Liang Jiang, Ming-Wen Zhao

Key Laboratory of Microbiological Engineering of Agricultural Environment, Ministry of Agriculture, and Department of Microbiology, College of Life Sciences, Nanjing Agricultural University, Nanjing, Jiangsu, People's Republic of China

ABSTRACT

Heat stress (HS) influences the growth and development of organisms. Thus, a comprehensive understanding of how organisms sense HS and respond to it is required. *Ganoderma lucidum*, a higher basidiomycete with bioactive secondary metabolites, has become a potential model system due to the complete sequencing of its genome, transgenic systems, and reliable reverse genetic tools. In this study, we found that HS inhibited mycelium growth, reduced hyphal branching, and induced the accumulation of ganoderic acid biosynthesis and heat shock proteins (HSPs) in *G. lucidum*. Our data showed that HS induced a significant increase in cytosolic Ca^{2+} concentration. Further evidence showed that Ca^{2+} might be a factor in the HS-mediated regulation of hyphal branching, ganoderic acid (GA) biosynthesis, and the accumulation of HSPs. Our results further showed that the calcium-permeable channel gene (*cch*)-silenced and phosphoinositide-specific phospholipase gene (*plc*)-silenced strains reduced the HS-induced increase in HSP expression compared with that observed for the wild type (WT). This study demonstrates that cytosolic Ca^{2+} participates in heat shock signal transduction and regulates downstream events in filamentous fungi.

IMPORTANCE

***Ganoderma lucidum*, a higher basidiomycete with bioactive secondary metabolites, has become a potential model system for evaluating how environmental factors regulate the development and secondary metabolism of basidiomycetes. Heat stress (HS) is an important environmental challenge. In this study, we found that HS inhibited mycelium growth, reduced hyphal branching, and induced HSP expression and ganoderic acid biosynthesis in *G. lucidum*. Further evidence showed that Ca^{2+} might be a factor in the HS-mediated regulation of hyphal branching, GA biosynthesis, and the accumulation of HSPs. This study demonstrates that cytosolic Ca^{2+} participates in heat shock signal transduction and regulates downstream events in filamentous fungi. Our research offers a new way to understand the mechanism underlying the physiological and metabolic responses to other environmental factors in *G. lucidum*. This research may also provide the basis for heat shock signal transduction studies of other fungi.**

Ganoderma lucidum, a traditional precious medicinal mushroom, has been commonly used throughout China and Southeast Asia for many centuries as a home remedy for treating minor disorders and promoting vitality and longevity (1). Modern pharmacological and clinical research has demonstrated that *G. lucidum* has significant antitumor, antiviral, antihypertensive, and immunomodulatory activities (2, 3). These pharmaceutical activities come from the bioactive compounds of *G. lucidum*. In recent years, many of these biologically useful compounds, including ganoderic acids (GAs) and polysaccharides, have been isolated and characterized in *G. lucidum* (4, 5). Ganoderic acids, also called triterpenoids, are one of the major secondary metabolites with pharmacological activity and are also known to be an important medicinal index found in *G. lucidum* (6). Previous studies have focused on the isolation and structural determination of GA and have attempted to understand the mechanisms underlying their action (4), but less work has been conducted to evaluate their biosynthesis. Several researchers have demonstrated the key biosynthetic enzyme genes in GA biosynthesis (7, 8). Some researchers have also reported that adding inducers, such as acetic acid and methyl jasmonate, in medium can increase GA accumulation (9, 10). However, the scarcity of basic biological studies has hindered the further development of *G. lucidum* and its commercial clinical use. Recently, the complete genome sequence (11), transgenic system (12), and reliable reverse genetic tools of *G. lucidum* were gradually developed (13), offering opportunities for further basic biological studies. Furthermore, as a higher basidiomycete with bioactive secondary metabolites, *G. lucidum* has become a potential model system for evaluating how environmental factors regulate the development and secondary metabolism of basidiomycetes.

Organisms are constantly challenged by ever-changing variables in their environment, and heat stress (HS) is one important environmental challenge. Microorganisms have a fixed way of life, as they cannot move to avoid environmental stress or regulate

Received 5 April 2016 **Accepted** 25 April 2016

Accepted manuscript posted online 29 April 2016

Citation Zhang X, Ren A, Li M-J, Cao P-F, Chen T-X, Zhang G, Shi L, Jiang A-L, Zhao M-W. 2016. Heat stress modulates mycelium growth, heat shock protein expression, ganoderic acid biosynthesis, and hyphal branching of *Ganoderma lucidum* via cytosolic Ca^{2+}. Appl Environ Microbiol 82:4112–4125. doi:10.1128/AEM.01036-16.

Editor: A. A. Brakhage, HKI and University of Jena

Address correspondence to Ming-Wen Zhao, mwzhao@njau.edu.cn.

X.Z. and A.R. contributed equally to this work.

Supplemental material for this article may be found at http://dx.doi.org/10.1128/AEM.01036-16.

body temperature to resist harsh environments, so HS can be especially severe for them. Many studies have reported the influence of HS on microorganisms. High temperatures decrease the survival rate of *Saccharomyces cerevisiae* (14), and in *Candida albicans*, fatty acid synthesis and membrane fluidity are tightly regulated in response to temperature (15). In higher basidiomycetes, Lu et al. reported that the fruit body growth of *Agaricus bisporus* was severely reduced in both pileus diameter and biomass after this mushroom suffered from high temperature for several days (16). With regard to the effects of HS on the development of fungi, further studies have revealed that the rapid protective transcriptional program, including heat shock proteins (HSPs) and heat shock factors (HSFs), plays a vital role in the heat stress response (HSR). In *S. cerevisiae*, this molecular defense is relatively clear (17). Among the most abundantly expressed HSPs are the highly conserved families of molecular chaperones, including HSP100, HSP90, HSP70, HSP60, and small HSPs (sHSPs), based on their molecular mass (18). Under HS conditions, the Hsp70 and Hsp90 chaperone systems have led the way in identifying the important cochaperones that play a vital role in blocking denatured protein aggregation, helping damaged proteins to fold, or dissolving the denatured proteins (19, 20). Furthermore, small HSPs, such as HSP26 and HSP42, play a vital role in promoting protein solubility when HS leads to general cytosolic protein unfolding (21). In most fungi, the increased expression of HSPs in a stressed cell is mediated primarily by heat shock factors (HSFs) (22).

Several studies have also identified certain signaling molecules that participate in the HSR in fungi. In *S. cerevisiae*, Cowart et al. illustrated that sphingolipids play a vital role in regulating translation under HS (23). In *Pleurotus eryngii*, a higher basidiomycete, Kong et al. reported that NO may serve as a signaling molecule to alleviate oxidative damage induced by HS (24). These studies demonstrate that signaling molecules participate in the HSR in fungi, but their precise roles in HS signaling transduction remain unclear.

Overall, although many studies have reported the HSR in fungi, the detailed mechanisms are still not very clear. First, the studies have focused mainly on *S. cerevisiae* or other ascomycetes, and less work has been conducted with other filamentous fungi, especially in higher basidiomycetes, which have high commercial value. Second, the relationship between HSPs and other signaling molecules in the HSR of fungi is still not clear. Therefore, it is necessary to study the mechanism of the HSR in higher basidiomycetes. In this report, we studied the effect of HS on mycelium growth, hyphal branching, and GA biosynthesis in *G. lucidum* and also measured the transcriptional levels of HSPs during the HSR. Our study illustrates that the phenotypes induced by HS were regulated by cytosolic Ca^{2+}. Further evidence showed that under HS, different calcium sources may have contributed to the increase in cytosolic Ca^{2+} levels in *G. lucidum*. Our research offers a new way to understand the mechanism underlying the physiological and metabolic responses to other environmental factors in *G. lucidum*. This research may also provide the basis for heat shock signal transduction studies of other fungi.

MATERIALS AND METHODS

Fungal strains and growth conditions. The DH5α strain of *Escherichia coli* was used for plasmid amplification and was grown in Luria-Bertani media containing 100 μg ml^{-1} ampicillin or 50 μg ml^{-1} kanamycin, as required. *G. lucidum*, strain HG, was obtained from the culture collection of the Edible Fungi Institute, Shanghai Academy of Agricultural Science, Shanghai, China. The wild-type (WT), CK (the empty vector controls), *cch*-silenced, and *plc*-silenced *G. lucidum* strains were cultured at 28°C in potato dextrose broth (PDB) medium.

HS and chemical treatments. To evaluate the mycelial growth rate and hyphal branching after HS, the *G. lucidum* strains were cultured on potato dextrose agar (PDA) plates for 3 days and then exposed to 42°C for 0 min to 120 min, followed by 2 days of recovery at 28°C.

To evaluate the cytosolic Ca^{2+} levels and the transcriptional expression levels of HSPs and calcium-related genes, 5-day-old *G. lucidum* strains were heat stressed at 42°C in a temperature-controlled chamber for 0 min to 60 min.

To detect ganoderic acid (GA) and its mesostate, *G. lucidum* strains were cultured in PDA liquid cultures with shaking for 5 days and then exposed to 42°C for 0 to 24 h until the 7th day at 28°C in stationary PDA liquid cultures. In the experiments in which 1,2-bis(o-aminophenoxy)ethane-*N*,*N*,*N*′,*N*′-tetraacetic acid (BAPTA), BAPTA-acetoxymethyl (AM), EGTA, $LaCl_3$, or neomycin was used, *G. lucidum* strains were incubated with the concentrations of BAPTA, BAPTA-AM, EGTA, $LaCl_3$, or neomycin indicated in the figure legends for 30 min before HS treatment. In the experiments requiring readdition of exogenous calcium, 2 mM $CaCl_2$ was used to supplement the specimens after EGTA pretreatment for 30 min.

Construction of RNAi plasmids and strains. As previously described (13), the dual-promoter-silencing vector pAN7-dual, driven by the glyceraldehyde-3-phosphate dehydrogenase (*gpd*) promoter and 35S promoter, was used to suppress the expression of *cch* or *plc*. The coding region of *cch* or *plc* was amplified by PCR, using *G. lucidum* cDNA as a template, with the primers listed in Table S1 in the supplemental material. The *cch* or *plc* fragment was doubly digested with KpnI and SpeI and inserted into the plasmid pAN7-dual after KpnI/SpeI restriction digestion. The RNA interference (RNAi)-silencing vectors pAN7-dual-cchi and pAN7-dual-plci, containing the hygromycin phosphotransferase-encoding gene (*hph*), were transferred into *G. lucidum* with electroporation, and the transformants were selected on CYM (1% maltose, 2% glucose, 0.2% yeast extract, 0.2% tryptone, 0.05% $MgSO_4 \cdot 7H_2O$, 0.46% KH_2PO_4) containing 100 μg/ml hygromycin B. Dozens of transformants were selected randomly, and real-time PCR analyses were used to suggest the silencing efficiency of these transformants. Two independent silencing strains with the highest silencing efficiency were selected for further study.

Real-time PCR analysis of gene expression. The levels of gene-specific mRNA expressed by the WT and isolated RNAi transformant strains were assessed using quantitative real-time PCR, according to our previous study (12). Gene expression was evaluated by calculating the difference between the threshold cycle (C_T) value of the gene analyzed and the C_T value of the housekeeping gene 18S rRNA. Post-reverse transcription-quantitative PCR (qRT-PCR) calculations analyzing the relative gene expression levels were performed according to the $2^{-\Delta\Delta CT}$ method described by Livak and Schmittgen (25). The gene fragments were amplified by real-time PCR using primers based on the *G. lucidum* genome sequence (11), as shown in Table S1 in the supplemental material.

Determining hyphal branching. Hyphal branching was measured as described by Mu et al. (26). Vegetative hyphae were removed from actively growing colonies, suspended in 2.5 μg ml^{-1} fluorescent brightener 28 (Sigma, USA), a fluorescent dye used for the staining of fungi, and viewed microscopically under a Nikon Eclipse Ti-S microscope (Nikon, Japan) with UV light. Images were recorded and processed using the NIS Elements F package (software developed by Nikon Corporation, Japan).

Free cytosolic Ca^{2+} labeling and detection. The free cytosolic Ca^{2+} localization pattern in the related media was monitored with the aid of Fluo-3AM, an acetoxymethyl ester of a fluorescent calcium indicator dye (Invitrogen). Fluo-3AM (50 μM) was loaded into cells by incubation at 37°C for 30 min, and the cells were then washed three times with phosphate-buffered saline (PBS). The Fluo-3AM-labeled cells were examined using a confocal laser scanning microscope (Leica model TCS SP2), ex-

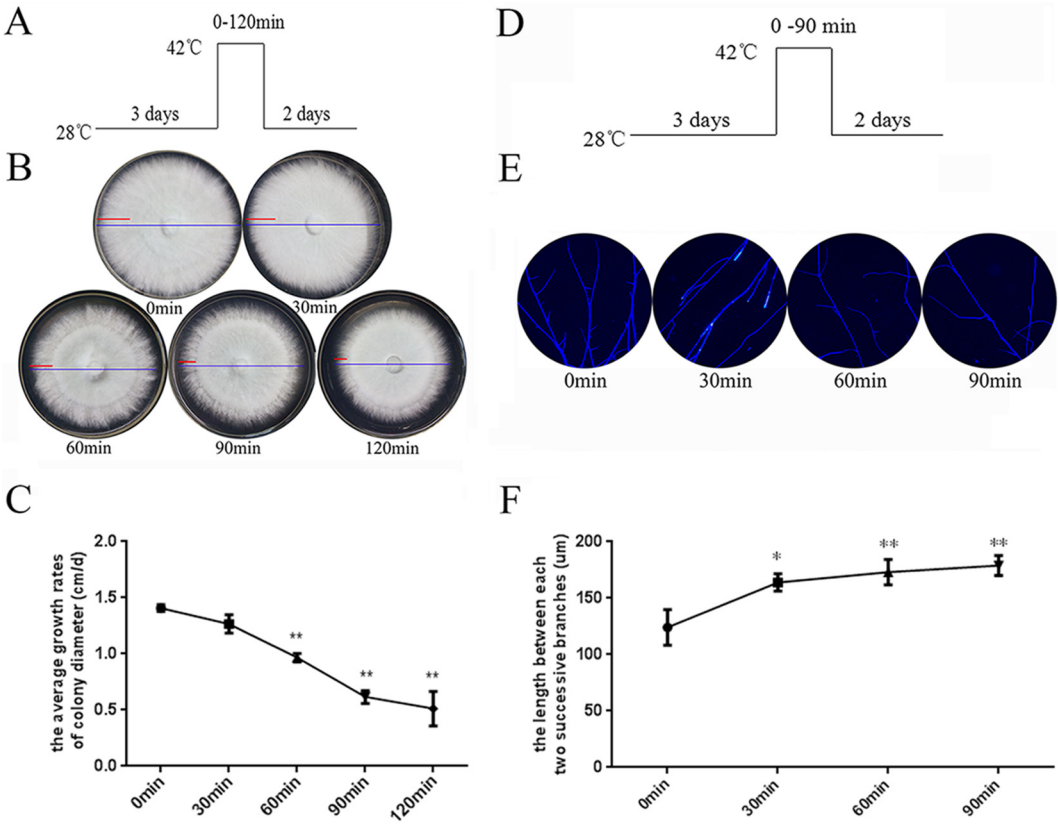

FIG 1 Inhibited growth and reduced hyphal branching in heat-stressed strains. (A) The *G. lucidum* wild-type strains were cultured on PDA plates for 3 days and then exposed to 42°C for 0 min to 120 min, followed by 2 days at 28°C. (B) The morphology of mycelial growth for the entire 5 days (blue line) and the following 2 days at 28°C after HS (red line) is shown. (C) The mycelial growth rate in centimeters per day was measured following 2 days at 28°C after HS and was subjected to statistical analysis. (D) The wild-type strains were cultured on PDA plates for 3 days and then exposed to 42°C for 0 min to 90 min, followed by 2 days at 28°C. (E) Vegetative hypha were removed from actively growing colonies, suspended in 2.5 μg ml^{-1} fluorescent brightener 28, and detected under a Nikon Eclipse Ti-S microscope with UV light. (F) Measurement of the length between two hyphal branches in *G. lucidum* with HS treatment. (C and F) Values are the means ± SD of the results from three independent experiments. Asterisks indicate significant differences from untreated strains (*, $P < 0.05$; **, $P < 0.01$, Student's *t* test).

cited at 488 nm with an Ar laser, and detected using a 505- to 530-nm band-pass filter. To eliminate the contribution of fluorescence background, control cells without Fluo-3AM labeling were also imaged under identical conditions.

Detection and measurement of GA and its mesostate in the GA biosynthesis pathway. Ganoderic acids were extracted from fungal mycelium and measured using a method described by Shi et al. (27). Briefly, 50 mg of dried mycelia was saponified for 2 h by treatment with 2 ml of 10% (wt/vol) KOH–75% (vol/vol) ethanol solution at 50°C. The mixture was extracted with hexane (2 ml) three times. The hexane layer was evaporated to dryness under N_2, and the residue was dissolved in 0.5 ml acetonitrile for the subsequent ultraperformance liquid chromatography (UPLC) analysis. An Agilent 1290 infinity UPLC equipped with an Agilent 1290 diode array detector and a 1.8-μm Agilent Zorbax Eclipse Plus C_{18} rapid-resolution high-definition column (2.1 by 50 mm) were used. The separation of squalene and lanosterol was achieved using a mobile phase of 100% methanol at a constant flow rate of 0.5 ml/min, and squalene and lanosterol were monitored at wavelengths of 195 and 210 nm, respectively. The peaks of squalene and lanosterol were identified based on their retention times and a comparison of the UV spectra with those obtained using squalene and lanosterol standards (Sigma, USA). The quantification was performed according to the external calibration peak areas versus the squalene and lanosterol concentration graphs obtained using standards.

Statistical analyses. All experiments were repeated at least three times with identical or similar results. The mean values from the individual experiments were expressed as means ± standard deviations (SD). Appropriate statistical tests are used for every figure. Student's *t* test was used for analyzing two compared samples. Duncan's multiple-range test was used for multiple comparisons. A *P* value of <0.05 was considered to be significant.

Accession number(s). The complete genome sequence of *G. lucidum* has been deposited in the GenBank database under accession number PRJNA71455.

RESULTS

Inhibited growth and reduced hyphal branching in heat-stressed strains. To evaluate how HS influences the growth of *G. lucidum*, wild-type *G. lucidum* strains were cultured on PDA plates for 3 days and then exposed to 42°C for 0 min to 120 min, followed by 2 days at 28°C (Fig. 1A). The mycelium morphology of *G. lucidum* after HS is shown in Fig. 1B; the blue line represents mycelium morphology for the entire 5 days, and the red line represents the 2 days at 28°C after HS. After HS for 60 min, the strains grew slowly and sparsely during recovery, and then a distinct "HS circle" formed. The strains treated with HS for 90 min and 120 min showed a lower growth rate during recovery. As shown in Fig. 1C, treatment with HS caused a 35% reduction in the mycelial growth rate in the heat-stressed strains (42°C for 60 min) compared with that of the untreated strains. Moreover, after HS for 90

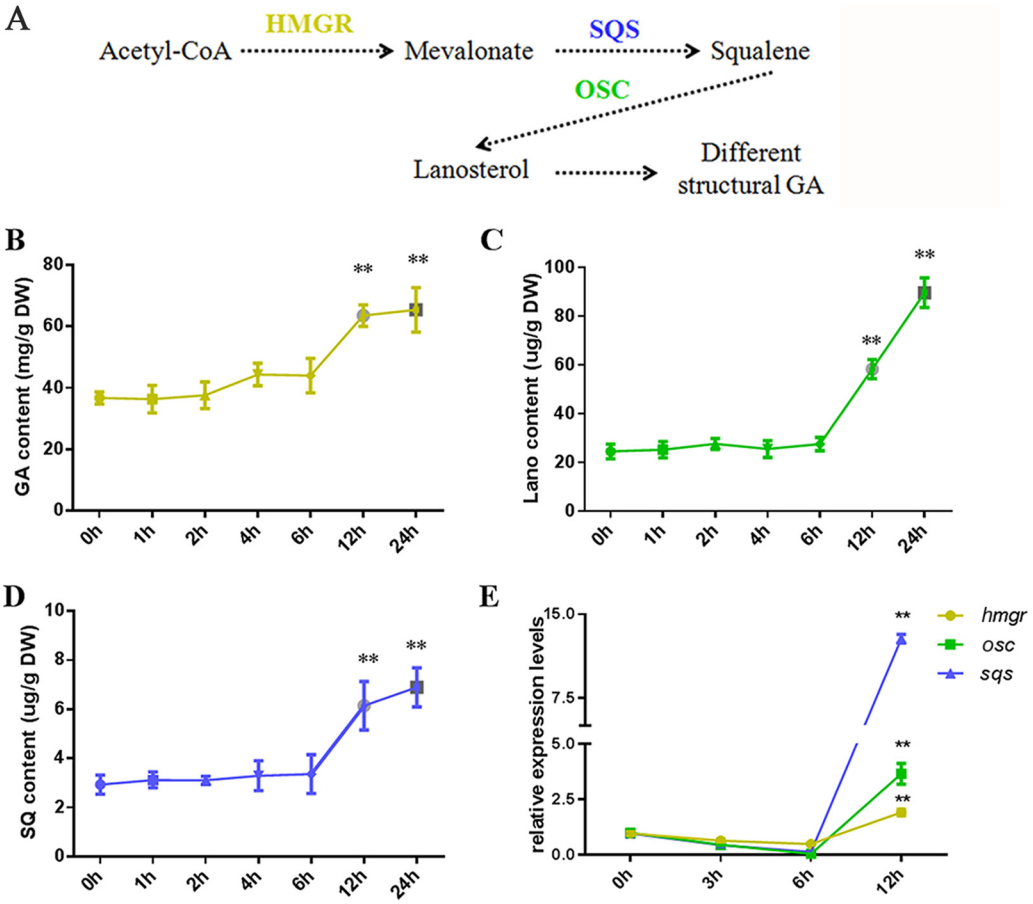

FIG 2 Increased GA biosynthesis in heat-stressed strains. (A) GA biosynthetic pathway of *G. lucidum*. Dashed lines indicate steps consisting of multiple enzyme reactions. HMGR, 3-hydroxy-3-methylglutaryl coenzyme A reductase; SQS, squalene synthase; OSC, oxidosqualene cyclase. The wild-type strains were cultured on PDA liquid cultures with shaking for 5 days, exposed to 42°C for 0 to 24 h, and monitored until the 7th day at 28°C in stationary PDA liquid cultures. The total GA (B), squalene (SQ) (C), and lanosterol (Lano) (D) contents were measured in the heat-stressed strains. (E) Relative expression of key enzyme genes of the GA biosynthetic pathway, *hmgr* (encoding 3-hydroxy-3-methylglutaryl coenzyme A reductase), *sqs* (encoding squalene synthase), and *osc* (encoding lanosterol synthase). The expression level of the *hmgr*, *sqs*, or *osc* gene from the wild-type strains without heat stress treatment was arbitrarily designated a value of 1. (B to E) Values are the means ± SD of the results from three independent experiments. Asterisks indicate significant differences from untreated strains (**, $P < 0.01$, Student's *t* test). DW, dry weight.

min and 120 min, the heat-stressed strains showed a severe reduction in the mycelial growth rate (50% and 55%, respectively). HS also caused a 36% and 42% reduction in mycelial dry weight in heat-stressed strains in liquid cultures (42°C for 12 h and 24 h, respectively) (see Fig. S1 in the supplemental material). Overall, after suffering from high temperatures, *G. lucidum* showed a reduced mycelial growth rate and decreased biomass.

Hyphal branching is an important indicator of the mycelium growth process of filamentous fungi (28); therefore, we evaluated hyphal branches after HS. As shown in Fig. 1E, we observed less hyphal branching in the heat-stressed strains for 30 min, 60 min, and 90 min. Quantitative results are shown in Fig. 1F; the length between two hyphal branches in *G. lucidum* treated with HS for 30 min showed a 1.23-fold increase compared to that without HS, and a 1.3- or 1.4-fold increase was observed for strains receiving 60 min or 90 min of HS, respectively. These results indicate that after HS, *G. lucidum* shows less hyphal branching.

Increased GA biosynthesis in heat-stressed strains. As a medicinal fungus, the secondary metabolites, and especially antitumor ganoderic acids (GAs), of *G. lucidum* have significant economic value. GAs are synthesized via the mevalonate pathway, in which acetyl coenzyme A (acetyl-CoA) is converted through a series of chemical reactions to mevalonate (MVA), to squalene, and, finally, to lanosterol. GAs then undergo a series of oxidation and reduction reactions before finally assuming the mature molecule structure (Fig. 2A). The GA levels were measured in the heat-stressed strains. As shown in Fig. 2B, the heat-stressed strains receiving 12 h and 24 h of treatment exhibited significant increases in GA content (increases of approximately 65% and 80%, respectively), whereas there were no significant differences in the GA contents between the strains that were heat stressed for 6 h and the untreated ones.

To monitor the metabolic process of GA biosynthesis, cellular squalene and lanosterol, two intermediate products of GA biosynthesis, were extracted and analyzed by ultraperformance liquid chromatography (UPLC). The squalene and lanosterol contents in the strains that were heat stressed for 12 h increased 1.9- and 2.0-fold, respectively, compared with those of the untreated strains (Fig. 2C and D). Additionally, HS for 24 h resulted in a 2.3- and 3.0-fold respective increases in squalene and lanosterol con-

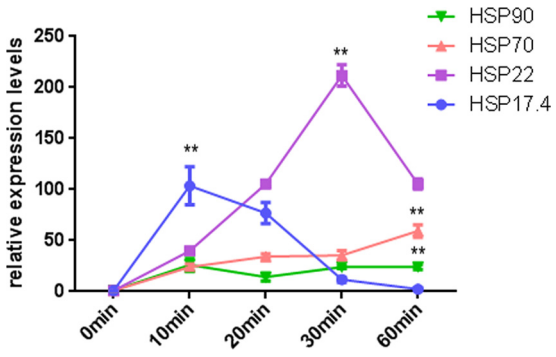

FIG 3 HS induced the upstream expression of HSPs. The wild-type strains were cultured on PDA plates for 5 days and then exposed to 42°C for 0 min to 60 min. The expression levels of the *hsp17.4* (A), *hsp22* (B), *hsp70* (C), and *hsp90* (D) genes were measured immediately after HS. The expression level of the *hsp17.4*, *hsp22*, *hsp70*, or *hsp90* gene from the wild-type strains without heat stress treatment was arbitrarily designated a value of 1. The values are the means ± SD of the results from three independent experiments. Asterisks indicate significant differences from untreated strains (**, $P < 0.01$, Student's *t* test).

tents (Fig. 2C and D). These results were consistent with those observed for the GA content.

Real-time quantitative RT-PCR was used to analyze the effects of HS on the expression of key enzyme genes of the GA biosynthetic pathway: *hmgr* (encoding 3-hydroxy-3-methylglutaryl coenzyme A reductase), *sqs* (encoding squalene synthase), and *osc* (encoding lanosterol synthase). The expression level of *hmgr* reached a 2-fold increase after HS for 12 h, and 3.5- and 13-fold increases were achieved in the expression levels of *sqs* and *osc*, respectively (Fig. 2E). Taken together, these data suggest that HS activates the expression of key enzyme genes of the GA biosynthetic pathway and then increases the GA, squalene, and lanosterol contents.

HS induced the upstream expression of HSPs. The HSR is characterized by the rapid reprogramming of gene expression, leading to a transient accumulation of HSPs that is correlated with enhanced thermotolerance (17). HSP70, HSP90, and some small molecular HSPs are among the most abundantly expressed HSPs. Using NCBI's Basic Local Alignment Search Tool (BLAST; http://blast.ncbi.nlm.nih.gov/Blast.cgi), the sequences of the *Dichomitus squalens* HSP17.4, HSP22, HSP70, and HSP90 genes were used to determine whether *G. lucidum* contains genes encoding HSP17.4, HSP22, HSP70, and HSP90. The phylogenetic analysis results are shown in Fig. S2 in the supplemental material. The data indicate that the phylogenetic relationship of HSP17.4, HSP22, HSP70, and HSP90 is closest between *G. lucidum* and *D. squalens*. The HSP genes of the ascomycetes and basidiomycetes had their own clusters. In our experiments, the transcription levels of *hsp17.4*, *hsp22*, *hsp70*, and *hsp90* substantially increased after HS (Fig. 3). The expression level of *hsp17.4* reached a maximum 110-fold increase at 10 min after the start of HS and then began to decrease at 20 min, returning to the initial level after 60 min (Fig. 3A). After HS, the expression level of *hsp22* reached a maximum 210-fold increase at 30 min (Fig. 3B), and a maximum 60-fold increase was achieved at 60 min for *hsp70* (Fig. 3C). The expression level of *hsp90* showed a 27-fold increase at 10 min after the start of HS and then began to decrease at 20 min (Fig. 3D). Taken together, *hsp17.4*, *hsp22*, *hsp70*, and *hsp90* responded to HS quickly and strongly, despite the differences in their optimal response times.

The cytosolic Ca^{2+} concentration was increased in heat-stressed strains. Ca^{2+} is widely used in prokaryotic and eukaryotic cells as a second messenger that triggers downstream signaling events when cells are exposed to environmental stress. High temperatures are known to trigger the generation of cytosolic Ca^{2+} in plants (29). The level of cytosolic Ca^{2+} was analyzed in 5-day-old strains grown at 28°C and then exposed to 42°C for 0 to 60 min. A stronger green fluorescence intensity was observed after HS for 10 min or 20 min than with the control, demonstrating that HS at 42°C induced an increase in the level of cytosolic Ca^{2+} (Fig. 4A). The start of this increase occurred within 10 min of the start of the HS. The fluorescence level emitted by the Ca^{2+}-activated fluorochrome reached a maximum 2.5-fold increase at 20 min after the start of the HS, followed by a 1.5-fold increase at 30 min, and then nearly returned to the initial level after 60 min (Fig. 4B). These results indicate that HS can increase the cytosolic Ca^{2+} content.

A systematic genomic analysis of the calcium signaling machinery in *G. lucidum* was also performed. A BLAST analysis indicated that 32 Ca^{2+}-signaling genes were found in *G. lucidum*; these included 22 genes regulating cytosolic Ca^{2+} concentration (1 phospholipase C gene [*plc*], 2 Ca^{2+}-permeable channel genes [*cch* and *mid*], 1 vacuole Ca^{2+} channel gene [*yvc*], 6 Ca^{2+} exchanger genes, and 12 Ca^{2+} pump genes) and 10 downstream genes responding to the Ca^{2+} signal (1 calcium-modulated protein [calmodulin] gene, 2 calcineurin [catalytic] genes, 1 calcineurin [regulatory] gene, 1 calcium binding protein [CABP] gene, 3 Ca^{2+} and CAM [calmodulin]-dependent protein kinase genes, 1 calreticulin/calnexin gene, and 1 calcineurin-responsive zinc [CRZ] finger transcription factor gene) (26). All of these Ca^{2+}-signaling genes are present in *Neurospora crassa*, *Magnaporthe grisea*, *S. cerevisiae*, and *Magnaporthe oryzae* (the most studied fungi with regard to Ca^{2+} signaling) (30, 31). Upon the application of HS, the transcriptional levels of the 32 Ca^{2+}-signaling genes were detected by using real-time quantitative RT-PCR (Fig. 4C). Under high temperatures, among the genes, most show little to no induction, with the exception of *plc*, *cch*, and a few others. The expression levels of *plc*, *cch*, and *yvc* reached 3.9-, 3.4-, and 3.7-fold increases at 10 min after the start of HS and then began to decrease at 20 min. At the same time, the transcriptional levels of *camk2*, *CNA1*, *CNA2*, and a few other downstream genes in the Ca^{2+} signal transduction pathway were also increased. Overall, HS increased the cytosolic Ca^{2+} content and activated the transcriptional levels of several Ca^{2+} channels and downstream Ca^{2+}-signaling-related genes.

Effect of Ca^{2+} inhibitors on the cytosolic Ca^{2+} concentration, hyphal branching, and GA biosynthesis in heat-stressed strains. To exclude the possibility that cytosolic Ca^{2+} might participate in the regulation of hyphal branching and GA biosynthesis, we employed various compounds that affect cytosolic Ca^{2+}, including the Ca^{2+} chelator EGTA and 1,2-bis(*o*-aminophenoxy)ethane-*N*,*N*,*N*′,*N*′-tetraacetic acid (BAPTA), a putative intracellular Ca^{2+} chelator (BAPTA-AM), a putative plasma membrane Ca^{2+} channel blocker ($LaCl_3$), and a phospholipase C inhibitor (neomycin). The results showed that when the strains were treated with these compounds, the level of cytosolic Ca^{2+} decreased compared with that in the control, which was only heat stressed (Fig. 5A). The quantitative results showed that treatment of the strains with BAPTA and EGTA (a putative extracellular

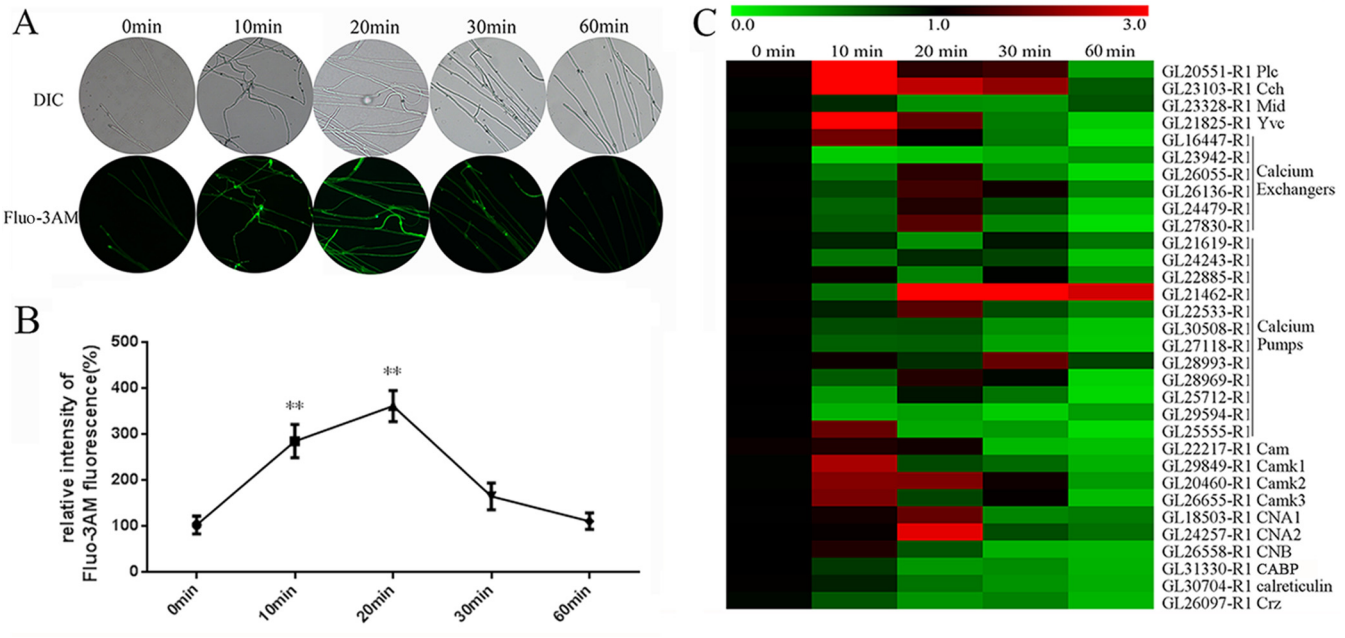

FIG 4 Cytosolic Ca^{2+} levels were increased in heat-stressed strains. (A) The wild-type strains were cultured on PDA plates for 5 days and then exposed to 42°C for 0 min to 60 min. For detection, 50 μM Fluo-3AM, a Ca^{2+} fluorescent probe, was used, and the intensity was monitored using confocal laser scanning microscopy (CLSM). Green fluorescence represents the free cytosolic Ca^{2+}. DIC, differential interference contrast. (B) Changes in the Ca^{2+} fluorescence ratio in the heat-stressed strains. The *y* axis is the Ca^{2+} fluorescence ratio measured by CLSM, and the *x* axis represents the different treatments. The values are the means ± SD of the results from three independent experiments. Asterisks indicate significant differences from untreated strains (**, $P < 0.01$, Student's *t* test). (C) Wild-type strains were cultured on PDA plates for 5 days and then exposed to 42°C for 0 min to 60 min. The expression levels of some Ca^{2+} signaling-related genes were measured immediately after HS. Relevant genes were detected using real-time PCR and were presented as a heat map generated using GENESPRINGGX 7.3.1 software (Agilent Technologies). The relative expression is shown as a mean value from 0.0 to 3.0 in green to red. The expression level of the Ca^{2+} signaling-related genes from the wild-type strains without heat stress treatment was arbitrarily designated a value of 1.0. Plc is GL20551-R1, Cch is GL23103-R1, Mid is GL23328-R1, Yvc is GL21825-R1, Cam is GL22217-R1, CamK1 is GL29849-R1, CamK2 is GL20460-R1, CamK3 is GL26655-R1, CNA1 is GL18503-R1, CNA2 is GL24557-R1, CNB is GL26558-R1, CABP is GL31330-R1, calreticulin is GL30704-R1, and Crz is GL25464-R1. Calcium exchangers include GL16447-R1, GL23942-R1, GL26055-R1, GL26136-R1, GL24479-R1, and GL27830-R1. Calcium pumps include GL21619-R1, GL24243-R1, GL22885-R1, GL21462-R1, GL22533-R1, GL30508-R1, GL27118-R1, GL28993-R1, GL28969-R1, GL25712-R1, GL29594-R1, and GL25555-R1.

Ca^{2+} chelator) led to a greater loss of cytosolic Ca^{2+} (60% and 80% reductions, respectively) (Fig. 5B). Strains treated with $LaCl_3$ (a putative plasma membrane Ca^{2+} channel blocker) had a 55% reduction in cytosolic Ca^{2+}. These results indicated that Ca^{2+} entry through the plasma membrane participated in the HS-induced increase in cytosolic Ca^{2+}. To investigate whether Ca^{2+} release from intracellular organelles also played a role in the HS-induced increase in cytosolic Ca^{2+}, we treated the strains with BAPTA-AM and neomycin. Treatment with BAPTA-AM (a putative intracellular Ca^{2+} chelator) and neomycin (a phospholipase C inhibitor) greatly decreased the content of HS-induced cytosolic Ca^{2+} compared with that in the control, which was only heat stressed (70% and 62% reductions, respectively) (Fig. 5B). These results suggested that HS can increase the cytosolic Ca^{2+} content and that these pharmacological blockers can be used to reduce the cytosolic Ca^{2+} concentration. Moreover, the different ways in which these compounds could reduce cytosolic Ca^{2+} levels also implied that different calcium sources participated in the increase in cytosolic Ca^{2+} levels in *G. lucidum* under HS.

Previous reports have shown that cytosolic Ca^{2+} participates in regulating hyphal branching in Nox-silenced strains of *G. lucidum* (26). To investigate whether hyphal branching is associated with cytosolic Ca^{2+} under HS, BAPTA, EGTA, $LaCl_3$, and neomycin were also employed to detect changes in hyphal branching. As shown in Fig. 5C, the length between two hyphal branches decreased when BAPTA, EGTA, $LaCl_3$, and neomycin were added. Quantitative results are shown in Fig. 5D; the length between two hyphal branches in *G. lucidum* following EGTA and BAPTA treatment decreased by 35% and 30%, respectively, compared with that in the control, which was only heat stressed (Fig. 5D). The effect of $LaCl_3$ and neomycin also caused 40% and 20% reductions, respectively, in the length between two hyphal branches compared with that in the control, which was only heat stressed. Overall, when BAPTA, EGTA, $LaCl_3$, and neomycin were used to decrease the content of HS-induced cytosolic Ca^{2+}, the length between two hyphal branches decreased compared with the length in the control, which was only heat stressed. These results indicate that HS-induced hyphal branching is regulated by cytosolic Ca^{2+}.

Our previous study revealed the effects of cytosolic Ca^{2+} on GA biosynthesis in Nox-silenced (26) and Gpx-silenced (32) strains. In this experiment, EGTA, $LaCl_3$, and neomycin were used to investigate the role of Ca^{2+} in regulating ganoderic acid biosynthesis under HS. As shown in Fig. 5E, treatment of the strains with these compounds led to reductions in the GA content compared with that of the control, which was only heat stressed. Among them, treatment with EGTA led to an 18% reduction in the GA content. Similarly, strains treated with $LaCl_3$ and neomycin had 50% and 20% reductions, respectively (Fig. 5E). The effects of these compounds on intermediate metabolites were consistent with GA biosynthesis. EGTA, $LaCl_3$, and neomycin resulted in

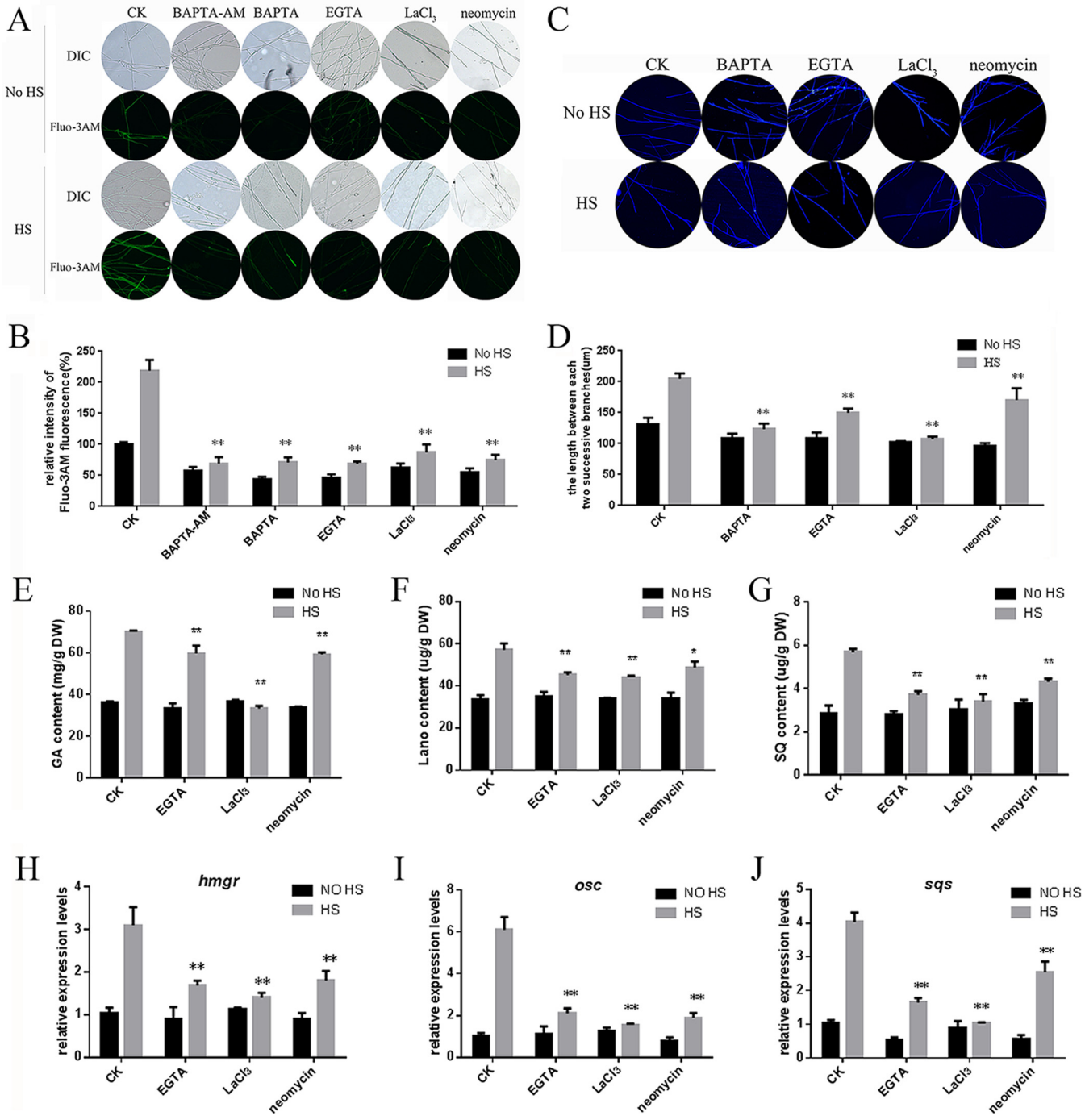

FIG 5 Effect of Ca^{2+} inhibitors on the cytosolic Ca^{2+} concentration, hyphal branching, and GA biosynthesis in heat-stressed strains. (A) To detect cytosolic Ca^{2+}, the wild-type strains were cultured on PDA plates for 5 days and then treated with 1 mM BAPTA-AM, 1 mM BAPTA, 5 mM EGTA, 10 mM $LaCl_3$, or 1 mM neomycin for 30 min. The strains were exposed to 42°C for 20 min. For detection, 50 μM Fluo-3AM, a Ca^{2+} fluorescent probe, was used, and the intensity was monitored using CLSM. Green fluorescence represents the free cytosolic Ca^{2+}. (B) Changes in the Ca^{2+} fluorescence ratio in the heat-stressed strains. (C) To detect hyphal branching, the wild-type strains were cultured on PDA plates for 3 days and then treated with 1 mM BAPTA, 5 mM EGTA, 10 mM $LaCl_3$, or 1 mM neomycin for 30 min. The strains were exposed to 42°C for 90 min, followed by 2 days at 28°C. Vegetative hypha were removed from actively growing colonies, suspended in 2.5 μg ml^{-1} fluorescent brightener 28, and detected under a Nikon Eclipse Ti-S microscope with UV light. (D) Measurement of the length between two hyphal branches in *G. lucidum* with HS treatment. (E to G) To detect GA biosynthesis, the wild-type strains were cultured on PDA liquid cultures for 5 days with shaking and then treated with 5 mM EGTA, 10 mM $LaCl_3$, or 1 mM neomycin for 30 min. The strains were exposed to 42°C for 12 h and followed until the 7th day at 28°C in stationary PDA liquid cultures. The total GA (E), lanosterol (F), and squalene (G) contents were measured in the heat-stressed strains. (H to J) Relative expression of key enzyme genes of the GA biosynthetic pathway. The values are the means ± SD of the results from three independent experiments. Asterisks indicate significant differences from the heat-stressed-only strains (*, $P < 0.05$; **, $P < 0.01$, Student's *t* test).

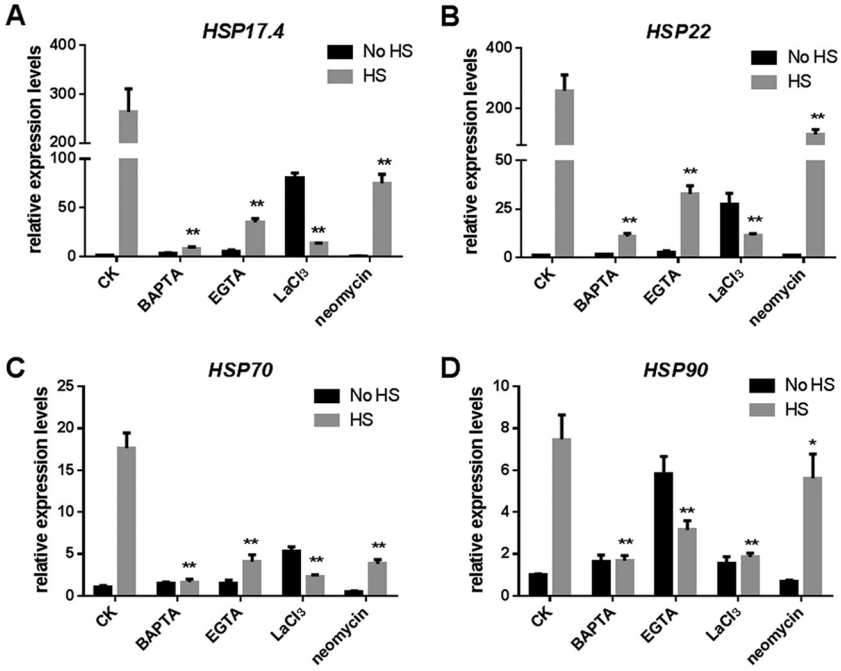

FIG 6 Effect of Ca^{2+} inhibitors on the expression of HSPs in heat-stressed strains. The wild-type strains were cultured on PDA for 5 days and then treated with 1 mM BAPTA, 5 mM EGTA, 10 mM $LaCl_3$, or 1 mM neomycin for 30 min. The strains were exposed to 42°C for 20 min. The expression levels of the *hsp17.4* (A), *hsp22* (B), *hsp70* (C), and *hsp90* (D) genes were measured immediately after HS. The values are the means ± SD of the results from three independent experiments. Asterisks indicate significant differences from the heat-stressed-only strains (*, $P < 0.05$; **, $P < 0.01$, Student's *t* test).

40%, 48%, and 32% reductions, respectively, in the squalene content in the heat-stressed strains (Fig. 5F). These compounds resulted in a nearly 20% reduction in the lanosterol content (Fig. 5G). Overall, when EGTA, $LaCl_3$, and neomycin were used to decrease the content of HS-induced cytosolic Ca^{2+}, the accumulation of GA biosynthesis was partially prevented.

The transcriptional levels of key enzyme genes of the GA biosynthetic pathway (*hmgr*, *sqs*, and *osc*) also decreased significantly when the strains were treated with EGTA, $LaCl_3$, and neomycin compared with levels in the control, which was only heat stressed. When the strains were treated with EGTA, $LaCl_3$, and neomycin, the expression level of *hmgr* was 50%, 60%, and 40% reduced, respectively (Fig. 5H). The expression level of *osc* was 60%, 70%, and 62% reduced, respectively, when treated with these compounds (Fig. 5I). EGTA, $LaCl_3$, and neomycin also caused 52%, 75%, and 37% reductions, respectively, in the expression level of *sqs* (Fig. 5J). These results showed that EGTA, $LaCl_3$, and neomycin could significantly decrease the HS-induced high expression levels of key enzyme genes of the GA biosynthetic pathway. Taken together, these data imply that Ca^{2+} participates in regulating HS-induced GA and the intermediate metabolites.

Effect of Ca^{2+} inhibitors on HSP expression in heat-stressed strains. It has been reported that HS-induced cytosolic Ca^{2+} is essential to induce HSPs in rice (33). To investigate the role of Ca^{2+} in the activation of HSPs under HS, EGTA, BAPTA, $LaCl_3$, and neomycin were employed to detect changes in transcriptional levels of HSPs. Under HS, the addition of EGTA lowered the expression levels of the *hsp17.4* gene by 84%, the *hsp22* gene by 90%, the *hsp70* gene by 78%, and the *hsp90* gene by 60% compared with their expression levels in the control, which was only heat stressed (Fig. 6). When BAPTA was added, the expression levels of the *hsp17.4*, *hsp22*, *hsp70*, and *hsp90* genes decreased by severalfold (>12-fold). Treatment with $LaCl_3$ resulted in a 96% reduction in the levels of expression of *hsp17.4* and *hsp22* and an 80% reduction for *hsp70* and *hsp90*. Meanwhile, the addition of neomycin lowered the expression level of the *hsp17.4* gene and the *hsp22* gene by 65%, the *hsp70* gene by 78%, and the *hsp90* gene by 30%. Taken together, when BAPTA, EGTA, $LaCl_3$, and neomycin were used to decrease the content of HS-induced cytosolic Ca^{2+}, the transcriptional levels of HSPs were also decreased. These results suggest that HS-induced HSP expression is regulated by cytosolic Ca^{2+}.

HS regulates hyphal branching and GA biosynthesis via cytosolic Ca^{2+}. To further elucidate the role of Ca^{2+} in regulating hyphal branching and GA biosynthesis under HS, we added exogenous $CaCl_2$ in the presence of EGTA in *G. lucidum*. Under HS, the addition of EGTA decreased cytosolic Ca^{2+} concentrations by 50% compared with concentrations in the control, which was only heat stressed (Fig. 7A and B). The readdition of $CaCl_2$ pretreated by EGTA could restore the cytosolic Ca^{2+} in the heat-stressed strains. Calcium-only treatments can increase cytosolic Ca^{2+} concentrations by 41% compared with those in the untreated strains. These results indicate that complementation of exogenous $CaCl_2$ could mostly restore the loss of cytosolic Ca^{2+} induced by EGTA under HS.

As shown in Fig. 7D, treatment with EGTA caused a 40% reduction in the length between two hyphal branches, but the readdition of $CaCl_2$ after pretreatment with EGTA could restore the length between two hyphal branches to that in the control, which was only heat stressed. Calcium-only treatments had no significant effect on hyphal branching compared with the untreated strains. These results suggest that hyphal branching is associated with cytosolic Ca^{2+} in *G. lucidum* under HS.

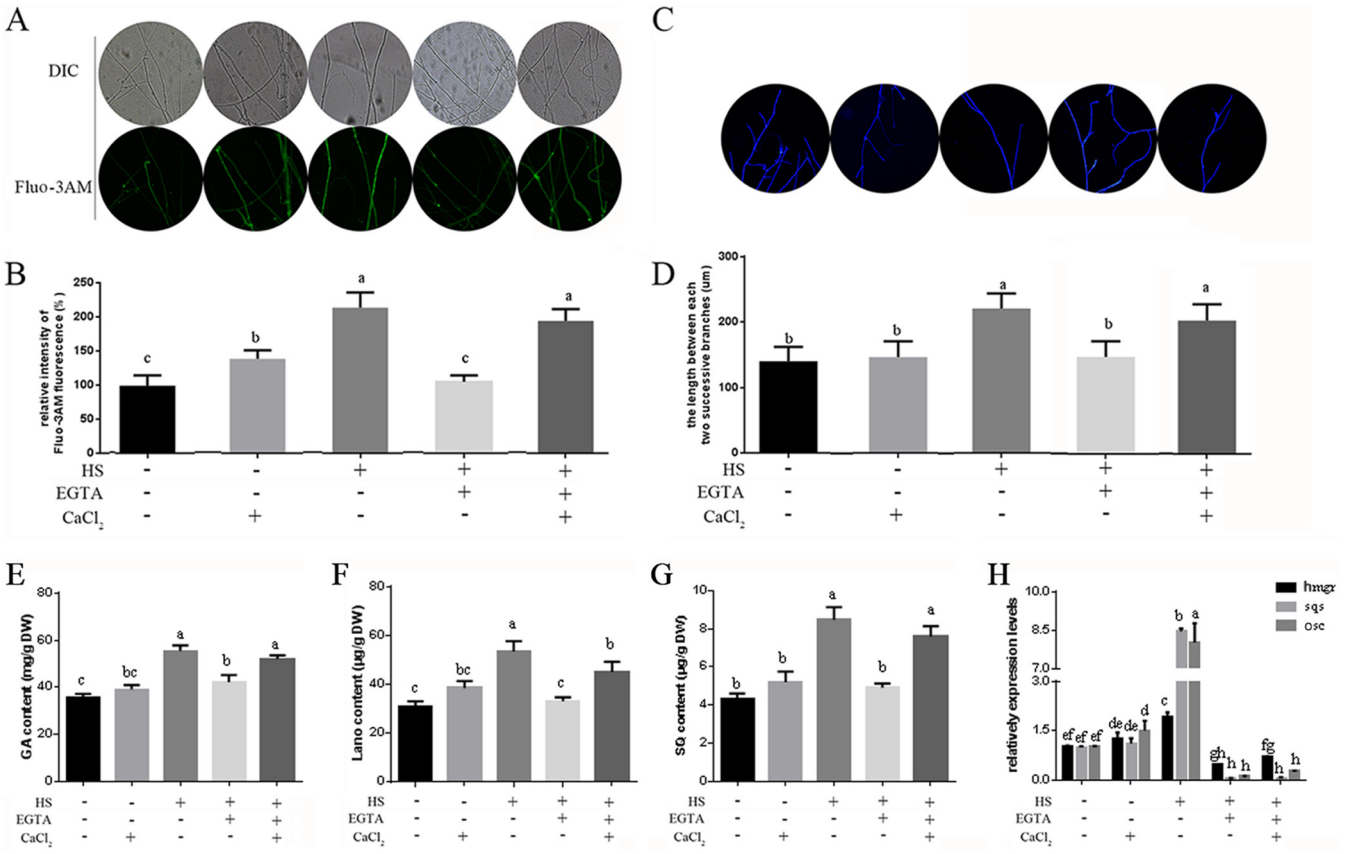

FIG 7 HS regulates hyphal branching and GA biosynthesis via cytosolic Ca^{2+}. (A) To detect cytosolic Ca^{2+}, the wild-type strains were cultured on PDA plates for 5 days and then treated in the presence (+) or absence (−) of 5 mM EGTA, with (+) or without (−) 2 mM $CaCl_2$ for 30 min. The strains were exposed to 42°C for 20 min, and then Fluo-3AM, a Ca^{2+} fluorescent probe, was used, and the intensity was monitored using CLSM. Green fluorescence represents the free cytosolic Ca^{2+}. (B) The *y* axis is the Ca^{2+} fluorescence ratio measured by CLSM, and the *x* axis represents the different treatments. (C) To detect hyphal branching, the wild-type strains were cultured on PDA plates for 3 days and then treated in the presence or absence of 5 mM EGTA, with or without 2 mM $CaCl_2$ for 30 min. The strains were exposed to 42°C for 90 min, followed by 2 days at 28°C. Vegetative hyphae were removed from actively growing colonies, suspended in 2.5 μg ml^{-1} fluorescent brightener 28, and detected under a Nikon Eclipse Ti-S microscope with UV light. (D) Measurement of the length between two hyphal branches in *G. lucidum* with HS treatment. (B to E) To detect GA biosynthesis, the wild-type strains were cultured on PDA liquid cultures for 5 days with shaking and then pretreated in the presence or absence of 5 mM EGTA, with or without 2 mM $CaCl_2$ for 30 min. These strains were exposed to 42°C for 12 h and monitored until the 7th day at 28°C in stationary PDA liquid cultures. Measurements of total GA (E), lanosterol (F), and squalene (G) contents in the heat-stressed strains are shown. (H) Relative expression of key enzyme genes of the GA biosynthetic pathway. Three repeated experiments were performed with similar results. The values are the means ± SD of the results from three independent experiments. Different letters indicate significant differences between the lines ($P < 0.05$, according to Duncan's multiple-range test).

The addition of EGTA lowered the GA contents by 22%, the lanosterol contents by 45%, and the squalene contents by 41% compared with the contents measured for the control, which was only heat stressed (Fig. 7E to G). However, when exogenous Ca^{2+} was supplemented, the GA, squalene, and lanosterol contents could be restored, despite the presence of EGTA. Calcium-only treatments had no significant effect on metabolite production compared with that in the untreated strains. The transcriptional levels of key enzyme genes of the GA biosynthetic pathway (*hmgr*, *sqs*, and *osc*) also decreased significantly when the strains were treated with EGTA compared with levels in the control, which was only heat stressed. However, the readdition of $CaCl_2$ after pretreatment with EGTA had no significant effect on the expression levels of *hmgr*, *sqs*, and *osc* (Fig. 7H). Overall, these results indicate that GA biosynthesis is associated with cytosolic Ca^{2+} under HS in *G. lucidum*.

HS regulates HSP expression via cytosolic Ca^{2+}. To further study the role of Ca^{2+} in regulating the accumulation of HSPs under HS, we added exogenous $CaCl_2$ in the presence of EGTA in *G. lucidum*. Under HS, treatment with EGTA caused 94%, 97%, 40%, and 65% reductions in the expression levels of the *hsp17.4*, *hsp22*, *hsp70*, and *hsp90* genes, respectively, compared with levels in the control, which was only heat stressed (Fig. 8). When exogenous Ca^{2+} was added, the expression levels of *hsp17.4*, *hsp22*, *hsp70*, and *hsp90* genes could mostly be restored to those of the control, which was only heat stressed. Calcium-only treatments can slightly increase the transcriptional level of *hsp90* but has no significant effect on the level of *hsp17.4*, *hsp22*, or *hsp70* compared with levels in the untreated strains. These results indicated that the modification of cytosolic Ca^{2+} levels under HS led to corresponding changes in HSP expression and suggest that cytosolic Ca^{2+} participates in regulating HSR in *G. lucidum*.

***cch* and *plc* participate in regulating HSP expression in *G. lucidum* under HS.** It is known that Ca^{2+} channels, pumps, and exchangers (carriers) control Ca^{2+} entry into and out of the cell and cellular compartments to maintain Ca^{2+} homeostasis and to

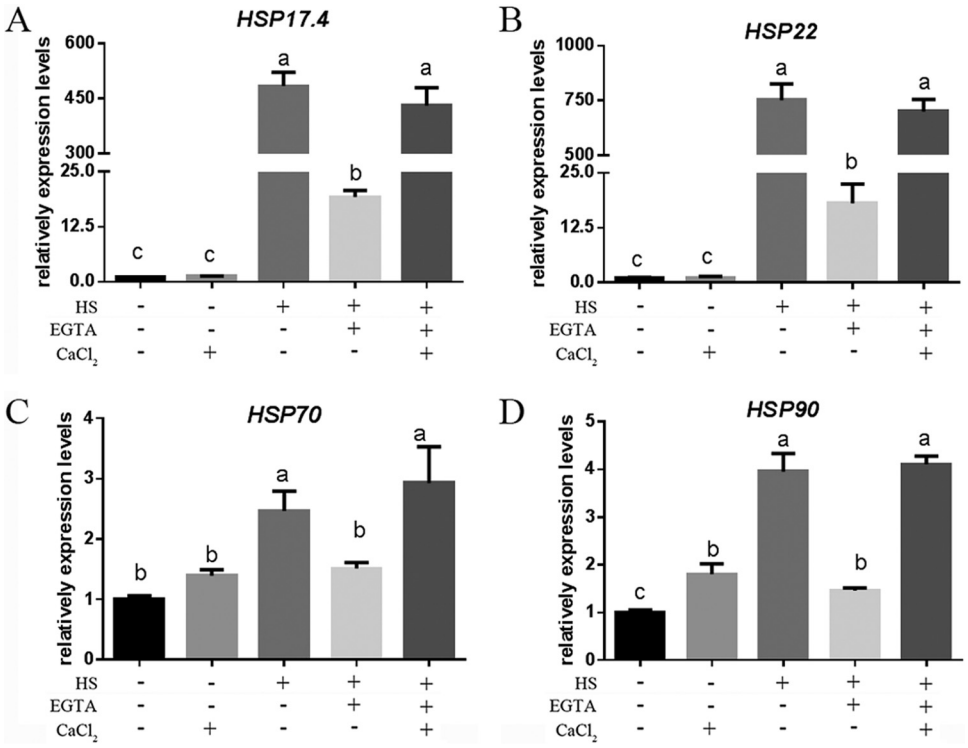

FIG 8 HS regulates HSP expression via cytosolic Ca^{2+}. The wild-type strains were cultured on PDA for 5 days and then treated in the presence (+) or absence (−) of 5 mM EGTA, with (+) or without (−) 2 mM $CaCl_2$ for 30 min. The strains were exposed to 42°C for 20 min. The expression levels of the *hsp17.4* (A), *hsp22* (B), *hsp70* (C), and *hsp90* (D) genes were measured immediately after HS. The values are the means ± SD of the results from three independent experiments. Different letters indicate significant differences between the lines ($P < 0.05$, according to Duncan's multiple-range test).

induce rapid signal-specific changes in cellular Ca^{2+} (34). Our previous study (Fig. 4C) showed that several genes regulating cytosolic Ca^{2+} concentrations had higher expression levels under HS than at normal temperatures, including the Ca^{2+}-permeable channel (*cch*) and phospholipase C (*plc*). Cch1p is a component of a high-affinity Ca^{2+}-permeable channel (35) and mediates calcium entry from extracellular stores (36). PLC regulates Ca^{2+} release from intracellular pools (37) and affects the thermotolerance of *Arabidopsis thaliana* by changing the cytosolic Ca^{2+} content and HSP expression (38). To further test whether Ca^{2+} regulates HSR under HS, we investigated the effects of *cch*- and *plc*-silenced strains on the increased cytosolic Ca^{2+} under HS. First, the sequences of the *S. cerevisiae cch* and *plc* genes were used to determine whether *G. lucidum* contains *cch* and *plc* genes using NCBI's BLAST (http://blast.ncbi.nlm.nih.gov/Blast.cgi). The results of phylogenetic analysis of Cch and PLC are shown in Fig. S3A and D in the supplemental material; the Cch and PLC of *G. lucidum* and other basidiomycetes have their own clusters. The RNAi silencing vector pAN7-dual (13) was used to express the sense-antisense structure of *cch* and *plc*. We constructed Cch-silencing and PLC-silencing vectors, named pAN7-dual-cchi (Fig. S3B) and pAN7-dual-plci (Fig. S3E), respectively, which carry the hygromycin B (Hyg) resistance gene as the selectable marker (Fig. S3). Real-time PCR analyses were used to suggest the silencing efficiency of the transformants, and Cch-silenced (cchi-6 and cchi-16) and PLC-silenced (plci-14 and plci-19) strains were selected for further analysis (Fig. S3C and F). Cch-silenced and PLC-silenced strains displayed thermosensitive phenotypes compared with the wild-type (WT) and empty vector (CK) strains after HS (Fig. S4). Upon application of HS, the *cch*-silenced strains had a 60% reduction in the cytosolic Ca^{2+} concentrations compared with that in the WT, and *plc*-silenced strains had a 58% reduction (Fig. S5). To test whether exogenous $CaCl_2$ could restore the loss of cytosolic Ca^{2+}, exogenous $CaCl_2$ was added. The results showed that under HS, Cch-silenced strains treated with exogenous Ca^{2+} caused only an 18% reduction in the cytosolic Ca^{2+} concentration compared with the concentration measured for the WT. The *plc*-silenced strains treated with exogenous Ca^{2+} caused only a 22% reduction in the Ca^{2+} concentration (Fig. S5B).

To further test the effect of cytosolic Ca^{2+} on HSR via a genetic approach, we investigated the effect of *cch*- and *plc*-silenced strains on the expression of HSPs under HS. Upon the application of HS, the *cch*-silenced strains caused 53%, 92%, 68%, and 63% reductions in the expression levels of the *hsp17.4*, *hsp22*, *hsp70*, and *hsp90* genes, respectively, compared with the levels measured for the WT. However, under HS, *cch*-silenced strains treated with exogenous Ca^{2+} caused only 30%, 25%, 33%, and 25% reductions in the expression levels of the *hsp17.4*, *hsp22*, *hsp70*, and *hsp90* genes, respectively (Fig. 9A to D). Upon application of HS, the *plc*-silenced strains treated with exogenous Ca^{2+} caused 27%, 34%, 31%, and 15% reductions in the expression levels of the *hsp17.4*, *hsp22*, *hsp70*, and *hsp90* genes, respectively, whereas the *plc*-silenced strains caused 70%, 73%, 57%, and 56% reductions, respectively, compared with the levels measured for the WT. These results demonstrate that the *cch*- and *plc*-silenced strains caused a reduction in the HS-induced increase in HSP expression compared with that measured for the WT. When external Ca^{2+} was added, the expression of HSPs was partly restored. These results indicate that under HS, *cch* and *plc* participate in regulating HSP

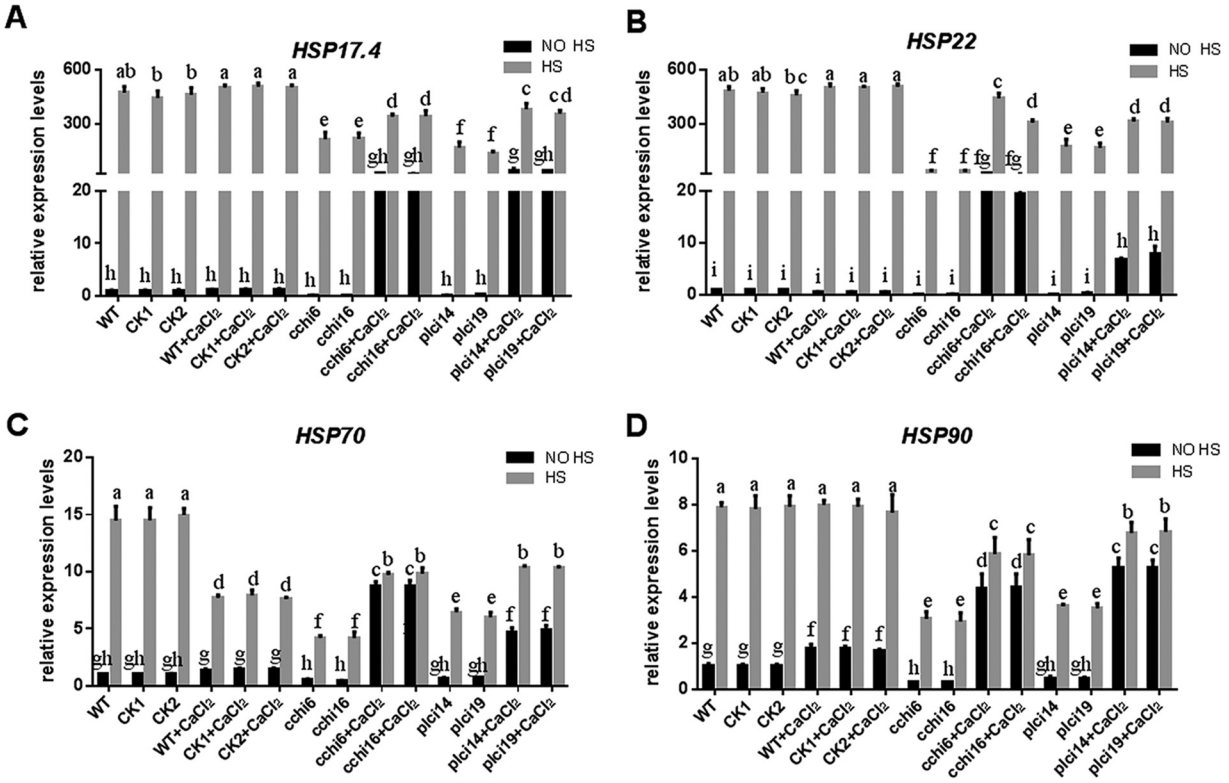

FIG 9 *cch* and *plc* participate in regulating HSP expression in *G. lucidum* under HS. The wild-type (WT), CK1, CK2 (transformed with the empty plasmid), *cch*-silenced (cchi6 and cchi16), and *plc*-silenced (plci14 and plci19) strains were cultured on PDA plates with or without 2 mM $CaCl_2$ for 5 days and then exposed to 42°C for 20 min. The expression levels of the *hsp17.4* (A), *hsp22* (B), *hsp70* (C), and *hsp90* (D) genes were measured immediately after HS. The expression level of the *hsp17.4*, *hsp22*, *hsp70*, or *hsp90* gene in the WT strain without heat stress and $CaCl_2$ treatment was arbitrarily designated a value of 1. The values are the means ± SD of the results from three independent experiments. Different letters indicate significant differences between the lines ($P < 0.05$, according to Duncan's multiple-range test).

expression. The genetic evidence is consistent with the pharmacological evidence, both of which suggest that under HS, cytosolic Ca^{2+} participates in regulating HSR. The findings further indicate that HS-induced cytosolic Ca^{2+} may have different sources.

DISCUSSION

HS is an important environmental stress that influences the growth and development of microorganisms. Thus, a comprehensive understanding of how microorganisms sense HS and respond to it is required. Although the HSR has been studied in considerable detail in bacteria and *Saccharomyces cerevisiae* (yeast), not all concepts elucidated there may apply to basidiomycetes due to their unique development and secondary metabolism. *G. lucidum*, a higher basidiomycete with bioactive secondary metabolites, has received much attention due to its commercial value. Therefore, the investigation of HS in *G. lucidum* is essential for foundational and applied research on the effects of HS on other large basidiomycetes.

Ca^{2+} is involved in the heat shock signal transduction pathway. Second messengers are intracellular signaling molecules released by the cell in response to extracellular signals. Ca^{2+} is the most important secondary messenger, connecting intracellular events with the extracellular environment and regulating many biological functions. Under specific conditions, such as exposure to environmental stress, the cytosolic Ca^{2+} transiently increases and activates downstream events. In rice, high temperature induced prolonged but transient increases in cytosolic Ca^{2+} (33). In *Physcomitrella*, a specific calcium-permeable channel was suggested to be the primary heat sensor and acted as a trigger for the appropriate transcriptional response that improves thermotolerance and cellular survival (39). Both of these studies showed that Ca^{2+} plays a role in heat shock signal transduction in plants. Our data show that HS induces a significantly increased cytosolic Ca^{2+} level in *G. lucidum*. Additionally, in our experiments, modification of cytosolic Ca^{2+} levels under HS led to corresponding changes in hyphal branching, GA biosynthesis, and HSP expression in *G. lucidum*. These mechanistic analyses show that upon application of HS, cytosolic Ca^{2+} participates in regulating the accumulation of HSPs, hyphal branching, and GA biosynthesis (Fig. 10). This study demonstrates that cytosolic Ca^{2+} participates in heat shock signal transduction in filamentous fungi. The mechanism of activation is similar to that in plants, suggesting that plants and fungi share a conserved mechanism of HS-activated cytosolic Ca^{2+}.

HS regulates hyphal branching and GA biosynthesis via cytosolic Ca^{2+}. Hyphal branching, which is closely related to the polar growth of filamentous fungi, is highly important for fungal development, reproduction, and pathogenicity (28), enables an increase in the surface area of the colony, and presumably enhances nutrient assimilation (40). Some researchers found that maintenance of hyphal branching is correlated with temperature. In *Aspergillus fumigatus*, higher temperatures induce greater hyphal elongation but poorer polar growth and reduced biofilm

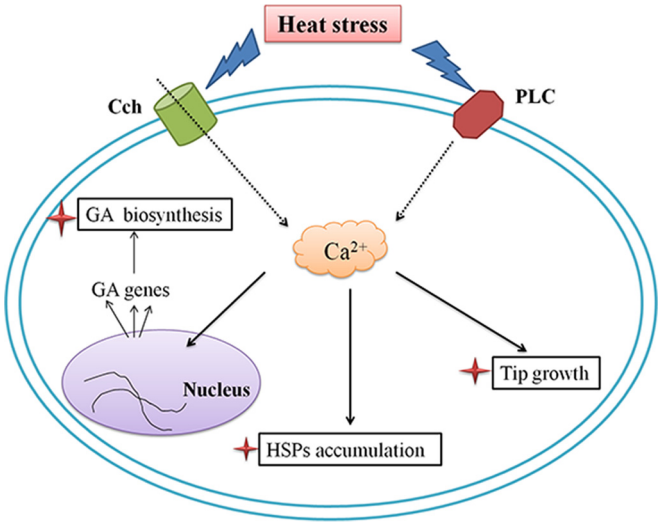

FIG 10 Schematic representation showing that HS regulates HSP expression, hyphal branching, and GA biosynthesis via cytosolic Ca^{2+} in *Ganoderma lucidum*. HS-induced cytosolic Ca^{2+} regulates GA biosynthesis, HSP accumulation, and hyphal branching. The black solid arrows indicate data supported by our own experiments, and the dotted arrows indicate data experimentally supported in other fungal systems.

thickness (41). In the white-rot fungus *Fomes* sp., high temperatures caused a decrease in mycelium branching but produced longer and thinner hyphae (42). Our data show that HS induces a lower growth rate and longer length between hyphal branches, which is similar to the results of previous studies.

The Ca^{2+} signal-mediated regulation of hyphal branching has also been reported in our previous study: UDP-glucose pyrophosphorylase (UGP) affected hyphal branching by regulating the cytosolic Ca^{2+} concentration (43), and Ca^{2+} regulated hyphal branching in Nox-silenced strains (26). However, Li et al. reported that reactive oxygen species (ROS), not cytosolic Ca^{2+}, have the greatest influence on hyphal branching in Gpx-silenced strains (32). In the present study, we found that Ca^{2+} might be the primary factor in the HS-mediated regulation of hyphal branching. This result is consistent with those of Mu et al. (26) and Li et al. (43); it also shows that the mechanism of hyphal branching is complex, as although the phenotype is the same, the mechanisms behind it may be different.

In a previous study, after suffering from high temperatures, sulfoquinovosylmonoacylglycerols (SQMG), sulfoquinovosyldiacylglycerols (SQDG), glycoalkaloids, and other secondary metabolites increased in *Nicotiana langsdorffii* (44). Similar results were shown in our study, where the GA content increased significantly in heat-stressed strains, and the levels of the intermediate products squalene and lanosterol also increased. Our previous study has revealed the effects of cytosolic Ca^{2+} on GA biosynthesis in Nox-silenced (26) and Gpx-silenced (32) strains. Our data also show that Ca^{2+} might be the primary factor in the HS-mediated regulation of GA biosynthesis, which further supports the role of Ca^{2+} in the regulation of biosynthesis of secondary metabolites in response to environmental stimuli.

HS regulates the accumulation of HSPs via cytosolic Ca^{2+}. The HSR is known to be universally conserved from bacteria to fungi. In the HSR of the model Gram-negative bacterium *Escherichia coli*, a large number of HSPs accumulate rapidly. Furthermore, in *Metarhizium anisopliae*, a filamentous fungus, Wang et al. demonstrated that HSPs play a vital role in the HSR (45). The function of these proteins has received a wide range of attention, but fewer studies have been performed to evaluate the relationship between these proteins and other signaling molecules in microorganisms (46). In this study, as expected, multiple genes encoding HSPs were significantly upregulated after HS. Further evidence showed that the accumulation of HSPs is regulated by cytosolic Ca^{2+} under HS. Similar phenomena have been reported in plants, specifically, that the increase in intracellular calcium triggers the accumulation of HSPs (47, 48). In the HS-induced transcription expression experiments, we found that several genes that regulate cytosolic Ca^{2+} concentration, including *plc*, *cch*, and *yvc*, had the highest expression levels at 10 min after the start of HS. Moreover, after HS, the cytosolic Ca^{2+} concentration reached a peak at 20 min, and most of the detected HSPs have an optimal response time at 30 min or 60 min. These findings imply that HS triggers calcium channel or calcium exchangers and then leads to a rapid and transient elevation in cytosolic Ca^{2+} concentration. Subsequently, a synthesis of different HSP mRNAs occurs. Taken together with the genetic evidence, these data imply that *cch* and *plc* participate in regulating HSP expression under HS, and they further indicate that cytosolic Ca^{2+} is involved in HSR. However, there are many genes that regulate the cytosolic Ca^{2+} concentration. HS-induced cytosolic Ca^{2+} may have different sources; whether other calcium channels participate in the HSR requires further study.

In summary, HS resulted in decreased mycelium growth, less hyphal branching, the upstream expression of HSPs, and the accumulation of ganoderic acids in *G. lucidum*. Furthermore, HS-induced cytosolic Ca^{2+} participated in heat shock signal transduction and regulated growth and metabolic biosynthesis. Further evidence showed that Ca^{2+} might be a factor in the HS-mediated regulation of hyphal branching, GA biosynthesis, and the accumulation of HSPs. Our results further indicate that under HS, *cch* and *plc* participate in regulating HSP expression.

ACKNOWLEDGMENTS

This work was supported by the National Natural Science Foundation of China (grants 31400035 and 31301825), the Fundamental Research Funds for the Central Universities (grant KJQN201527), the Science & Technology Pillar Program of Jiangsu Province, China (grant BE2015361), and the Chinese National Key Technology R&D Program (grant 2013BAD20B05).

FUNDING INFORMATION

This work, including the efforts of Ang Ren, was funded by Fundamental Research Funds for the Central Universities (KJQN201527). This work, including the efforts of Ming-Wen Zhao, was funded by Science and Technology Pillar Program of Jiangsu Province, China (BE2015361). This work, including the efforts of Ming-Wen Zhao, was funded by Chinese National Key Technology R&D Program (2013BAD20B05). This work, including the efforts of Ang Ren, was funded by National Natural Science Foundation of China (NSFC) (31400035). This work, including the efforts of Ai-Liang Jiang, was funded by National Natural Science Foundation of China (NSFC) (31301825).

REFERENCES

1. **Mizushina Y, Hanashima L, Yamaguchi T, Takemura M, Sugawara F, Saneyoshi M, Matsukage A, Yoshida S, Sakaguchi K.** 1998. A mushroom fruiting body-inducing substance inhibits activities of replicative DNA

polymerases. Biochem Biophys Res Commun **249:**17–22. http://dx.doi.org/10.1006/bbrc.1998.9091.
2. **Calviño E, Manjon JL, Sancho P, Tejedor MC, Herraez A, Diez JC.** 2010. *Ganoderma lucidum* induced apoptosis in NB4 human leukemia cells: involvement of Akt and Erk. J Ethnopharmacol **128:**71–78. http://dx.doi.org/10.1016/j.jep.2009.12.027.
3. **Yue QX, Song XY, Ma C, Feng LX, Guan SH, Wu WY, Yang M, Jiang BH, Liu X, Cui YJ, Guo DA.** 2010. Effects of triterpenes from *Ganoderma lucidum* on protein expression profile of HeLa cells. Phytomedicine **17:**606–613. http://dx.doi.org/10.1016/j.phymed.2009.12.013.
4. **Paterson RR.** 2006. *Ganoderma*—a therapeutic fungal biofactory. Phytochemistry **67:**1985–2001. http://dx.doi.org/10.1016/j.phytochem.2006.07.004.
5. **Liu RM, Li YB, Zhong JJ.** 2012. Cytotoxic and pro-apoptotic effects of novel ganoderic acid derivatives on human cervical cancer cells *in vitro*. Eur J Pharmacol **681:**23–33. http://dx.doi.org/10.1016/j.ejphar.2012.02.007.
6. **Shi L, Ren A, Mu D, Zhao M.** 2010. Current progress in the study on biosynthesis and regulation of ganoderic acids. Appl Microbiol Biotechnol **88:**1243–1251. http://dx.doi.org/10.1007/s00253-010-2871-1.
7. **Zhao MW, Liang WQ, Zhang DB, Wang N, Wang CG, Pan YJ.** 2007. Cloning and characterization of squalene synthase (SQS) gene from *Ganoderma lucidum*. J Microbiol Biotechnol **17:**1106–1112.
8. **Shang CH, Zhu F, Li N, Ou-Yang X, Shi L, Zhao MW, Li YX.** 2008. Cloning and characterization of a gene encoding HMG-CoA reductase from *Ganoderma lucidum* and its functional identification in yeast. Biosci Biotechnol Biochem **72:**1333–1339. http://dx.doi.org/10.1271/bbb.80011.
9. **Ren A, Qin L, Shi L, Dong X, Mu DS, Li YX, Zhao MW.** 2010. Methyl jasmonate induces ganoderic acid biosynthesis in the basidiomycetous fungus *Ganoderma lucidum*. Bioresour Technol **101:**6785–6790. http://dx.doi.org/10.1016/j.biortech.2010.03.118.
10. **Ren A, Li XB, Miao ZG, Shi L, Jaing AL, Zhao MW.** 2014. Transcript and metabolite alterations increase ganoderic acid content in *Ganoderma lucidum* using acetic acid as an inducer. Biotechnol Lett **36:**2529–2536. http://dx.doi.org/10.1007/s10529-014-1636-9.
11. **Chen S, Xu J, Liu C, Zhu Y, Nelson DR, Zhou S, Li C, Wang L, Guo X, Sun Y, Luo H, Li Y, Song J, Henrissat B, Levasseur A, Qian J, Li J, Luo X, Shi L, He L, Xiang L, Xu X, Niu Y, Li Q, Han MV, Yan H, Zhang J, Chen H, Lv A, Wang Z, Liu M, Schwartz DC, Sun C.** 2012. Genome sequence of the model medicinal mushroom *Ganoderma lucidum*. Nat Commun **3:**913. http://dx.doi.org/10.1038/ncomms1923.
12. **Shi L, Qin L, Xu Y, Ren A, Fang X, Mu D, Tan Q, Zhao M.** 2012. Molecular cloning, characterization, and function analysis of a mevalonate pyrophosphate decarboxylase gene from *Ganoderma lucidum*. Mol Biol Rep **39:**6149–6159. http://dx.doi.org/10.1007/s11033-011-1431-9.
13. **Mu D, Shi L, Ren A, Li M, Wu F, Jiang A, Zhao M.** 2012. The development and application of a multiple gene co-silencing system using endogenous *URA3* as a reporter gene in *Ganoderma lucidum*. PLoS One **7:**e43737. http://dx.doi.org/10.1371/journal.pone.0043737.
14. **Gibney PA, Lu C, Caudy AA, Hess DC, Botstein D.** 2013. Yeast metabolic and signaling genes are required for heat-shock survival and have little overlap with the heat-induced genes. Proc Natl Acad Sci U S A **110:**E4393–E4402. http://dx.doi.org/10.1073/pnas.1318100110.
15. **Leach MD, Cowen LE.** 2014. Membrane fluidity and temperature sensing are coupled via circuitry comprised of Ole1, Rsp5, and Hsf1 in *Candida albicans*. Eukaryot Cell **13:**1077–1084. http://dx.doi.org/10.1128/EC.00138-14.
16. **Lu Z, Kong X, Lu Z, Xiao M, Chen M, Zhu L, Shen Y, Hu X, Song S.** 2014. *Para*-aminobenzoic acid (PABA) synthase enhances thermotolerance of mushroom *Agaricus bisporus*. PLoS One **9:**e91298. http://dx.doi.org/10.1371/journal.pone.0091298.
17. **Verghese J, Abrams J, Wang Y, Morano KA.** 2012. Biology of the heat shock response and protein chaperones: budding yeast (*Saccharomyces cerevisiae*) as a model system. Microbiol Mol Biol Rev **76:**115–158. http://dx.doi.org/10.1128/MMBR.05018-11.
18. **Morano KA, Grant CM, Moye-Rowley WS.** 2012. The response to heat shock and oxidative stress in *Saccharomyces cerevisiae*. Genetics **190:**1157–1195. http://dx.doi.org/10.1534/genetics.111.128033.
19. **Vogel M, Mayer MP, Bukau B.** 2006. Allosteric regulation of Hsp70 chaperones involves a conserved interdomain linker. J Biol Chem **281:**38705–38711. http://dx.doi.org/10.1074/jbc.M609020200.
20. **Taipale M, Jarosz DF, Lindquist S.** 2010. HSP90 at the hub of protein homeostasis: emerging mechanistic insights. Nat Rev Mol Cell Biol **11:**515–528. http://dx.doi.org/10.1038/nrm2918.
21. **Cashikar AG, Duennwald M, Lindquist SL.** 2005. A chaperone pathway in protein disaggregation. Hsp26 alters the nature of protein aggregates to facilitate reactivation by Hsp104. J Biol Chem **280:**23869–23875.
22. **Meyer U, Monnerjahn C, Techel D, Rensing L.** 2000. Interaction of the *Neurospora crassa* heat shock factor with the heat shock element during heat shock and different developmental stages. FEMS Microbiology Lett **185:**255–261. http://dx.doi.org/10.1111/j.1574-6968.2000.tb09071.x.
23. **Cowart LA, Gandy JL, Tholanikunnel B, Hannun YA.** 2010. Sphingolipids mediate formation of mRNA processing bodies during the heat-stress response of *Saccharomyces cerevisiae*. Biochem J **431:**31–38. http://dx.doi.org/10.1042/BJ20100307.
24. **Kong W, Huang C, Chen Q, Zou Y, Zhang J.** 2012. Nitric oxide alleviates heat stress-induced oxidative damage in *Pleurotus eryngii* var. *tuoliensis*. Fungal Genet Biol **49:**15–20. http://dx.doi.org/10.1016/j.fgb.2011.12.003.
25. **Livak KJ, Schmittgen TD.** 2001. Analysis of relative gene expression data using real-time quantitative PCR and the 2(−Delta Delta C(T)) method. Methods **25:**402–408. http://dx.doi.org/10.1006/meth.2001.1262.
26. **Mu D, Li C, Zhang X, Li X, Shi L, Ren A, Zhao M.** 2014. Functions of the nicotinamide adenine dinucleotide phosphate oxidase family in *Ganoderma lucidum*: an essential role in ganoderic acid biosynthesis regulation, hyphal branching, fruiting body development, and oxidative-stress resistance. Environ Microbiol **16:**1709–1728. http://dx.doi.org/10.1111/1462-2920.12326.
27. **Shi L, Gong L, Zhang X, Ren A, Gao T, Zhao M.** 2015. The regulation of methyl jasmonate on hyphal branching and GA biosynthesis in *Ganoderma lucidum* partly via ROS generated by NADPH oxidase. Fungal Genet Biol **81:**201–211. http://dx.doi.org/10.1016/j.fgb.2014.12.002.
28. **Harris SD, Momany M.** 2004. Polarity in filamentous fungi: moving beyond the yeast paradigm. Fungal Genet Biol **41:**391–400. http://dx.doi.org/10.1016/j.fgb.2003.11.007.
29. **Saidi Y, Finka A, Goloubinoff P.** 2011. Heat perception and signalling in plants: a tortuous path to thermotolerance. New Phytol **190:**556–565. http://dx.doi.org/10.1111/j.1469-8137.2010.03571.x.
30. **Zelter A, Bencina M, Bowman BJ, Yarden O, Read ND.** 2004. A comparative genomic analysis of the calcium signaling machinery in *Neurospora crassa*, *Magnaporthe grisea*, and *Saccharomyces cerevisiae*. Fungal Genet Biol **41:**827–841. http://dx.doi.org/10.1016/j.fgb.2004.05.001.
31. **Nguyen QB, Kadotani N, Kasahara S, Tosa Y, Mayama S, Nakayashiki H.** 2008. Systematic functional analysis of calcium-signalling proteins in the genome of the rice-blast fungus, *Magnaporthe oryzae*, using a high-throughput RNA-silencing system. Mol Microbiol **68:**1348–1365. http://dx.doi.org/10.1111/j.1365-2958.2008.06242.x.
32. **Li C, Shi L, Chen D, Ren A, Gao T, Zhao M.** 2015. Functional analysis of the role of glutathione peroxidase (GPx) in the ROS signaling pathway, hyphal branching and the regulation of ganoderic acid biosynthesis in *Ganoderma lucidum*. Fungal Genet Biol **82:**168–180. http://dx.doi.org/10.1016/j.fgb.2015.07.008.
33. **Wu HC, Luo DL, Vignols F, Jinn TL.** 2012. Heat shock-induced biphasic Ca^{2+} signature and OsCaM1-1 nuclear localization mediate downstream signalling in acquisition of thermotolerance in rice (*Oryza sativa* L.). Plant Cell Environ **35:**1543–1557. http://dx.doi.org/10.1111/j.1365-3040.2012.02508.x.
34. **Cyert MS, Philpott CC.** 2013. Regulation of cation balance in *Saccharomyces cerevisiae*. Genetics **193:**677–713. http://dx.doi.org/10.1534/genetics.112.147207.
35. **Liu M, Du P, Heinrich G, Cox GM, Gelli A.** 2006. Cch1 mediates calcium entry in *Cryptococcus neoformans* and is essential in low-calcium environments. Eukaryot Cell **5:**1788–1796. http://dx.doi.org/10.1128/EC.00158-06.
36. **Peiter E, Fischer M, Sidaway K, Roberts SK, Sanders D.** 2005. The *Saccharomyces cerevisiae* Ca^{2+} channel Cch1pMid1p is essential for tolerance to cold stress and iron toxicity. FEBS Lett **579:**5697–5703. http://dx.doi.org/10.1016/j.febslet.2005.09.058.
37. **Kiselyov K, Xu X, Mozhayeva G, Kuo T, Pessah I, Mignery G, Zhu X, Birnbaumer L, Muallem S.** 1998. Functional interaction between InsP3 receptors and store-operated Htrp3 channels. Nature **396:**478–482. http://dx.doi.org/10.1038/24890.
38. **Gao K, Liu YL, Li B, Zhou RG, Sun DY, Zheng SZ.** 2014. *Arabidopsis thaliana* phosphoinositide-specific phospholipase C isoform 3 (AtPLC3) and AtPLC9 have an additive effect on thermotolerance. Plant Cell Physiol **55:**1873–1883. http://dx.doi.org/10.1093/pcp/pcu116.

39. **Saidi Y, Finka A, Muriset M, Bromberg Z, Weiss YG, Maathuis FJ, Goloubinoff P.** 2009. The heat shock response in moss plants is regulated by specific calcium-permeable channels in the plasma membrane. Plant Cell **21:**2829–2843. http://dx.doi.org/10.1105/tpc.108.065318.
40. **Park HJ, Floss DS, Levesque-Tremblay V, Bravo A, Harrison MJ.** 2015. Hyphal branching during arbuscule development requires reduced arbuscular mycorrhiza1. Plant Physiol **169:**2774–2788.
41. **Zeng R, Li M, Chen Q, Wang L, Zhan P, Wang C, Lv G, Shen Y, Liu W.** 2014. *In vitro* analyses of mild heat stress in combination with antifungal agents against *Aspergillus fumigatus* biofilm. Antimicrob Agents Chemother **58:**1443–1450. http://dx.doi.org/10.1128/AAC.01007-13.
42. **Ordaz A, Favela E, Meneses M, Mendoza G, Loera O.** 2012. Hyphal morphology modification in thermal adaptation by the white-rot fungus *Fomes* sp. EUM1. J Basic Microbiol **52:**167–174. http://dx.doi.org/10.1002/jobm.201000528.
43. **Li M, Chen T, Gao T, Miao Z, Jiang A, Shi L, Ren A, Zhao M.** 2015. UDP-glucose pyrophosphorylase influences polysaccharide synthesis, cell wall components, and hyphal branching in *Ganoderma lucidum* via regulation of the balance between glucose-1-phosphate and UDP-glucose. Fungal Genet Biol **82:**251–263. http://dx.doi.org/10.1016/j.fgb.2015.07.012.
44. **Scalabrin E, Radaelli M, Rizzato G, Bogani P, Buiatti M, Gambaro A, Capodaglio G.** 2015. Metabolomic analysis of wild and transgenic *Nicotiana langsdorffii* plants exposed to abiotic stresses: unraveling metabolic responses. Anal Bioanal Chem **407:**6357–6368. http://dx.doi.org/10.1007/s00216-015-8770-7.
45. **Wang ZX, Zhou XZ, Meng HM, Liu YJ, Zhou Q, Huang B.** 2014. Comparative transcriptomic analysis of the heat stress response in the filamentous fungus *Metarhizium anisopliae* using RNA-Seq. Appl Microbiol Biotechnol **98:**5589–5597. http://dx.doi.org/10.1007/s00253-014-5763-y.
46. **Leach MD, Cowen LE.** 2013. Surviving the heat of the moment: a fungal pathogens perspective. PLoS Pathog **9:**e1003163. http://dx.doi.org/10.1371/journal.ppat.1003163.
47. **Finka A, Cuendet AF, Maathuis FJ, Saidi Y, Goloubinoff P.** 2012. Plasma membrane cyclic nucleotide gated calcium channels control land plant thermal sensing and acquired thermotolerance. Plant Cell **24:**3333–3348. http://dx.doi.org/10.1105/tpc.112.095844.
48. **Rodriguez-Caban J, Gonzalez-Velazquez W, Perez-Sanchez L, Gonzalez-Mendez R, Rodriguez-del Valle N.** 2011. Calcium/calmodulin kinase1 and its relation to thermotolerance and HSP90 in *Sporothrix schenckii*: an RNAi and yeast two-hybrid study. BMC Microbiol **11:**162. http://dx.doi.org/10.1186/1471-2180-11-162.